Optimization and Modeling of CuOx/OMWNT's for Catalytic Reduction of Nitrogen Oxides by Response Surface Methodology

Mahnaz Pourkhalil[*]

Assistance Professor, Nanotechnology Research Center, Research Institute of the Petroleum Industry, Tehran, Iran

Abstract

A series of copper oxide (CuOx) catalysts supported by oxidized multi-walled carbon nanotubes (OMWNT's) were prepared by the wet impregnation method for the low temperature (200 °C) selective catalytic reduction of nitrogen oxides (NOx) using NH_3 as a reductant agent in the presence of excess oxygen. These catalysts were characterized by FTIR, XRD, SEM-EDS, and H_2-TPR methods. The response surface methodology was employed to model and optimize the effective parameters in the preparation of CuOx/OMWNT's catalysts in NOx removal by NH_3-SCR process. Three experimental parameters, including calcination temperature, calcination time, and CuOx loading were chosen as the independent variables. The central composite design was utilized to establish a quadratic model as a functional relationship between the conversion of NOx as a response factor and independent variables. The ANOVA results showed that the NOx conversion is significantly affected by calcination temperature and CuOx loading. At the optimal values of the studied parameters, the maximum conversion of NOx, 86.3 %, was obtained at a calcination temperature of 318 °C, a calcination time of 3.4 hr., and CuOx loading of 16.73 wt.%; the reaction conditions was as follows: T= 200 °C, P= 1 bar, NO = NH_3 = 900 ppm, O_2 = 5 vol.%, and GHSV = 30,000 $hr.^{-1}$. The regression analysis with an R^2 value of 0.9908 revealed a satisfactory correlation between the experimental data and the values predicted for the conversion of NOx. The XRD and H_2-TPR results of the best catalyst showed that the formation of CuO as the dominant phase of CuOx is the key factor in low temperature selective catalytic reduction (SCR) process.

Keywords: CuOx/OMWNT's, Selective Catalytic Reduction, Nitrogen Oxides, Response Surface Methodology, Optimization

1. Introduction

NOx from power plants, waste incinerators, industrial boilers, engines, and automobiles has become the major source of air pollution, which results in ozone depletion, photochemical smog, acid rain, and green-house effects (Sun et al., 2017). Selective catalytic reduction (SCR) with NH_3 has been proven to be one of the most attractive techniques for NOx removal (Wu et al., 2018; Pourkhalil et al., 2018). V_2O_5-WO_3/TiO_2 commercial catalyst has been utilized for NH_3-SCR in the 300- 400 °C temperature range before dust removal instrument and desulfurizer equipment (Jung et al., 2017b; Jung et al., 2017a; Barreau et al., 2018). Due to the high concentration of SO_2 and ash dust in this location, the performance and life of the catalyst decreases intensively. There is a great interest in developing new SCR catalysts which are active at temperatures much below 300 °C, so the SCR unit can be placed in the downstream sections of the desulfurizer and electrostatic precipitators (Barreau et al., 2018; Fang et al., 2018). Carbon nanotubes (CNT's) are receiving attention as a catalyst support in

_____
* Corresponding Author:
    Email: pourkhalilm@ripi.ir

low-temperature SCR of NOx due to their high activity and good adsorption of NOx (Wang et al., 2013; Samojeden et al., 2015; Vermisoglou et al., 2011). MWNT's, having unique networks, tube shapes, and a mesoporous structure, are as an ideal support with a high surface area and good thermal and mechanical stability (Roe et al., 2017; Lv et al., 2017; Gangupomu et al., 2016). Moreover, copper oxide catalysts have been extensively investigated for the low-temperature SCR of NOx in works of Cu/ZSM-5 (Liu et al., 2016), Cu-Chabazite (Zhang et al., 2017), and Cu-SSZ-13 (Shan et al., 2017; Luo et al., 2017). However, few studies on CuOx-carbonaceous materials in NH_3–SCR are reported in the literature (Li et al., 2012). It is reported that CuO/activated carbon (Zhu et al., 2000) catalyst has a high activity at temperatures more than 180 °C. The purpose of the present study is to investigate the effects of various process parameters, including CuOx loading, calcination temperature, and calcination time of the CuOx catalysts supported on OMWNT's for the low-temperature SCR of NOx by NH_3 using the face-centered central composite design (FCCCD). The response surface methodology was utilized to investigate and predict the optimum values of the effective parameters for maximum NOx conversion. The catalysts were characterized by means of XRD, SEM, and H_2-TPR analyses.

2. Experimental

2.1. Catalyst preparation and characterization

a. Catalyst preparation

The raw MWNT's (95% purity, 10–30 nm in the outer diameter) were synthesized by a CVD method over a Co–Mo/MgO catalyst at Research Institute of the Petroleum Industry, Iran (Kibria et al., 2004). After the purification of the synthesized MWNT's, they were oxidized in a 1:3 (v/v) solution of HNO_3 (65%) and H_2SO_4 (98%) in an ultrasonic bath maintained at 60 °C for 2 hrs (Xing et al., 2005; Pourkhalil et al., 2013) to introduce the oxygenated surface groups onto the walls of MWNT's. These functional groups are helpful for anchoring and dispersing metal oxide species uniformly on the MWNT's surfaces (Chuang et al., 2011; Sedaghatzadeh et al., 2012). Then, the solution was filtered and washed using de-ionized H_2O, and it was finally dried in an oven at 100 °C in air for 24 hrs. A series of supported copper oxide catalysts at different loadings (4–24 wt.%) were synthesized by the wet impregnation technique. The OMWNT's were impregnated by a certain volume of an aqueous solution of Cu $(NO_3)_2 \cdot 6H_2O$ (analytical reagent, Merck) as the precursor for copper oxide under vigorous stirring at 60 °C for 2 hrs. The solutions were dried in a rotary evaporator at 78 °C and in an oven at 100 °C for 24 hrs respectively. The loading of copper oxide on the OMWNT's was controlled by adjusting the ratio of the OMWNT's to copper nitrate. The catalysts were calcined in a tubular furnace at different temperatures (300-700 °C) and at different times (2-10 hrs) in an atmosphere of helium at a flow rate of 50 mL.min^{-1} to obtain CuOx/OMWNT's catalysts.

b. Catalyst characterization

The FTIR spectra of the MWNT's and OMWNT's were reordered on a Thermo Nicolet Nexus-670 in KBr pellets ranging from 500 to 4000 cm^{-1}. The crystalline phase of the samples was examined by an X-ray diffraction analyzer. The measurements were obtained by a MPD-PHILIPS XRD instrument with Cu Ka ($k = 1.5056$ Å) in the range of 5 to 70°. The uniformity of the metal oxide dispersion over the surface of the support was characterized by a scanning electron microscope (SEM, Philips model XL30) operated at 120 keV. The TPR experiments were performed on a Micromeritics-2900 system connected to a thermal conductivity detector. For each test, 50 mg of the sample was exposed to 5% H_2 in Argon at a flow rate of 40 cc.min^{-1} from 50 to 700 °C.

2.2. Catalytic activity tests

The SCR activity tests were performed in a U-tube fixed-bed reactor with an inside diameter of 6 mm. The experiments were performed under atmospheric pressure at 200 °C, and 300 mg catalyst was used in each test; the total flow rate was also maintained at 600 mL.min^{-1}. The gas composition was 900 ppm NO, 900 ppm NH_3, and 5 vol.% O_2 balanced by helium. NO, NO_2, and O_2 concentrations in the

feed and product lines were controlled using an on-line gas analyzer (Testo model 340, Germany) equipped with $NO/NO_2/O_2$ sensors at each testing point. The reaction temperature was measured by a K-type thermocouple attached to the sample holder. The catalytic conversion (*X*) was calculated by the following Equation:

$$X\,(\%) = \frac{[NO]in - [NO]out}{[NO]in} \times 100 \tag{1}$$

2.3. Statistical analysis

The response surface methodology based on central composite design is one of the strongest mathematical and statistical techniques which can be used to design experiments, build empirical models, evaluate the effects of independent variables, and predict targeted responses (Badday et al., 2013; Danmaliki et al., 2017; Hosseini et al., 2017). Herein, a central composite design with three-level values was employed to investigate the effects of metal oxide loading, calcination temperature, and calcination time of CuOx/OMWNT's catalysts on the NOx removal rate as the response function in an NH_3-SCR process. The interaction effects and optimal parameters were obtained by Design Expert 7.0 software. Based on three independent variables by the software, two extreme points (the highest and the lowest) were used for each factor: 300 and 700 °C for calcination temperature (X_1), 2 and 10 hrs for calcination time (X_2), and 4 and 24 wt.% for CuOx loading (X_3) (see Table 1). For convenience, all these variables are symbolized as A, B, and C respectively.

Table 1

Range of independent variables and the experimental domain.

Factor	Name	Low (-1)	Middle (0)	High (+1)
A (X_1)	Calcination temperature (°C)	300	500	700
B (X_2)	Calcination time (hr.)	2	6	10
C (X_3)	CuOx loading (wt.%)	4	14	24

A total of 20 experiments, including 8 cube points, 6 center points in the cube, and 6 axial points were performed in this study (Kumar and Singh, 2014). All the experiments were performed randomly to minimize the impact of unaccountable variance in the response function caused by unrelated parameters. The CCD matrix was constructed as given in Table 2.

Table 2

The CCD matrix of the experimental and yield response.

Run	Independent variables (uncoded and coded)			Y-responses (NOx conversion)	
	A	B	C	Experimental	Predicted
1	300(-1)	6(0)	14(0)	86	84
2	500(0)	6(0)	14(0)	74	74.8
3	300(-1)	2(-1)	4(-1)	31	33.2
4	500(0)	10(+1)	14(0)	68	68.8
5	500(0)	6(0)	14(0)	76	74.8
6	300(-1)	2(-1)	24(+1)	78	79.8
7	700(+1)	10(+1)	24(+1)	29	31.18

	Independent variables (uncoded and coded)			Y-responses (NOx conversion)	
Run	A	B	C	**Experimental**	**Predicted**
8	700(+1)	6(0)	14(0)	46	52.9
9	500(0)	6(0)	14(0)	73.5	74.8
10	300(-1)	10(+1)	4(-1)	34	36
11	500(0)	6(0)	14(0)	75	74.8
12	500(0)	2(-1)	14(0)	71	75.1
13	700(+1)	10(+1)	4(-1)	5	7.3
14	500(0)	6(0)	14(0)	71	74.8
15	500(0)	6(0)	4(-1)	32	30.2
16	500(0)	6(0)	14(0)	72	74.8
17	700(+1)	2(-1)	24(+1)	44	46.5
18	500(0)	6(0)	24(+1)	58	65.4
19	300(-1)	10(+1)	24(+1)	62	67
20	700(+1)	2(-1)	4(-1)	8	7.2

The experimental results of CCD were fitted to a second-order quadratic polynomial model to predict the response function as follows (Equation (2)):

$$Y = b_0 + \sum_{i=1}^{n} b_i X_i + \sum_{i=1}^{n} b_{ii} X_i^2 + \sum_{i=1}^{n} \sum_{j>1}^{n} b_{ij} X_i X_j \qquad (2)$$

where, Y is the response function, and X_i and X_j are considered as the independent variables. b_0 (constant), b_i (linear), b_{ii} (quadratic), and b_{ij} (second order) terms are the regression coefficients, and n is the number of the total independent factors.

3. Results and discussion

3.1. Characterization of CuOx/OMWNT's catalysts

Figures 1a and b present the FTIR spectra of the MWNT's and OMWNT's to display the introduction of oxygenated groups onto the walls of carbon nanotubes by the acid treatment. The weak peaks at 1170 and 1575 cm^{-1} in the IR spectra of the MWNT's (Figure 1a) originate from the stretching mode of carbon-carbon bands in the raw MWNT's (Liu et al., 2005). Figure 1b shows the absorption peaks at 1300-1400, 1715, and 3430 cm^{-1} attributed to carbonyl (C-O), carboxyl (C=O), and hydroxyl (O-H) groups respectively (Bazarganipour and Salavati-Niasari, 2016; Jiang and Gao, 2003). This shows that the oxygenated groups have been created in the walls of the OMWNT's by the sonochemical acid treatment. Increasing the peak intensity at 1170 and 1575 cm^{-1} over OMWNT's (Figure 1b) is assigned to the asymmetric stretching of C=C due to introducing the oxygenated groups. The presence of a small peak at 3430 cm^{-1} over MWNT's (Figure 1a) corresponds to the acid purification process of the raw MWNT's (Pourkhalil et al., 2013).
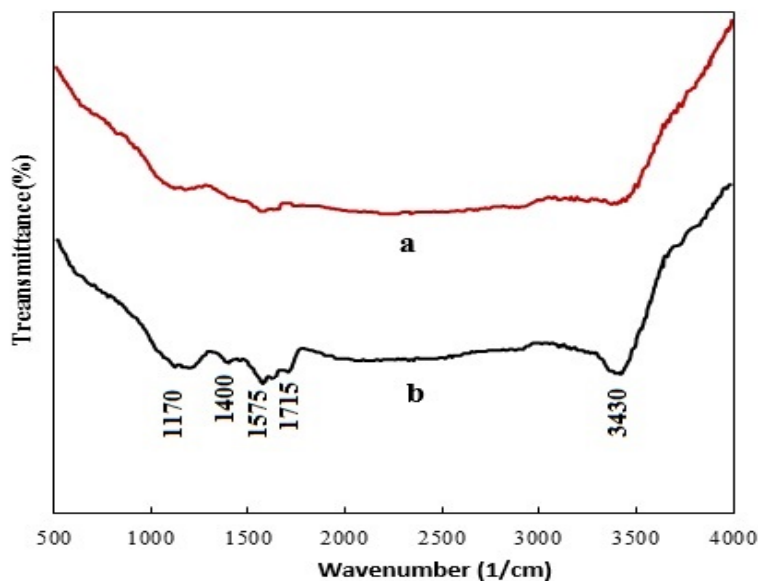
Figure 1

FT-IR spectra of (a) MWNT's and (b) OMWNT's.

Figure 2 shows the XRD patterns of the OMWNT's and 14 wt.% CuOx/OMWNT's calcined at 300, 500, and 700 °C for 3 hrs. In Figure 2a, the peaks at 2θ of 25.7, 41.9, and 43.16 ° from the (002), (100), and (101) graphite diffractions (JCPDS # 08-0415) show that the structure of the MWNT's support was not destroyed through the acid treatment (Belin and Epron, 2005). When the calcination temperature was 300 °C, only a few diffraction peaks for CuO (JCPDS # 80-1916) were observed (Figure 2b). After increasing the calcination temperature from 300 to 500 °C (Figure 2c), the crystal phase of Cu_2O (JCPDS#05-0667) became apparent and the intensity of the CuO peaks decreased. Finally, at 700 °C, the diffraction peaks of Cu_2O increased slightly, and the peaks of copper metal (JCPDS # 85-1326) appeared (Figure 2d).
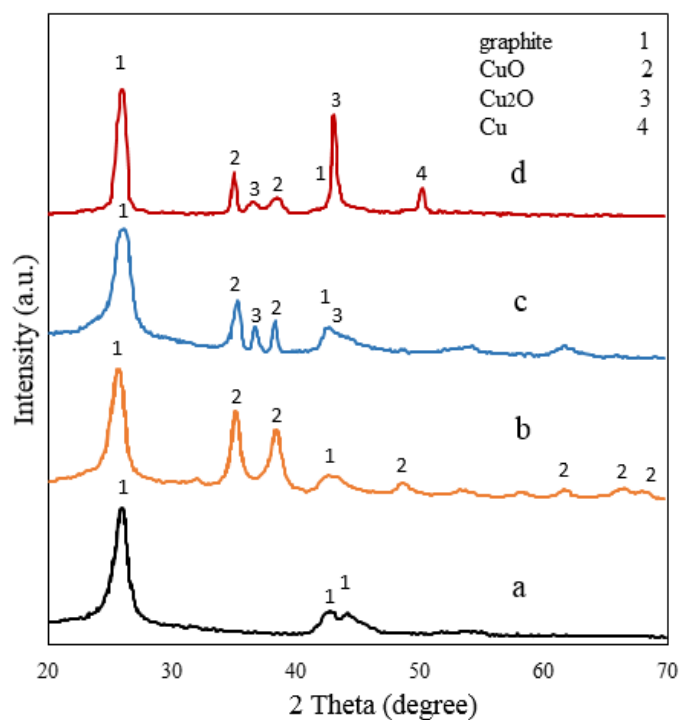

Figure 2

XRD patterns of a) OMWNT's, and 14 wt.% CuOx/OMWNT's calcined at (b) 300 °C, c) 500 °C, and d) 700 °C.

The H_2-TPR analysis of the catalysts calcined at different temperatures (300 to 700 °C) was performed to investigate their reducibility and recognize the metal species of the CuOx/OMWNT's catalysts. As shown in Figure 3a, two peaks of H_2 consumption were observed on the profile of the catalyst calcined at 300 °C. The peaks centered at 250 and 465 °C are attributed to the reduction of Cu^{2+} to Cu^+ and Cu^+ to Cu^0 respectively (Wan et al., 2004). As shown in Figures 3b and c, the second peak located at about 460 °C was enhanced compared to the first peak because of increasing the number of Cu^+ ions over the catalysts via calcination temperature increasing from 500 to 700 °C. It can be seen that increasing the calcination temperature from 300 to 700 °C (Figures 3a to 3c) reduced the Cu^{+2} ions (the first peak) as well as the reducibility of the catalysts at temperatures lower than 350 °C.
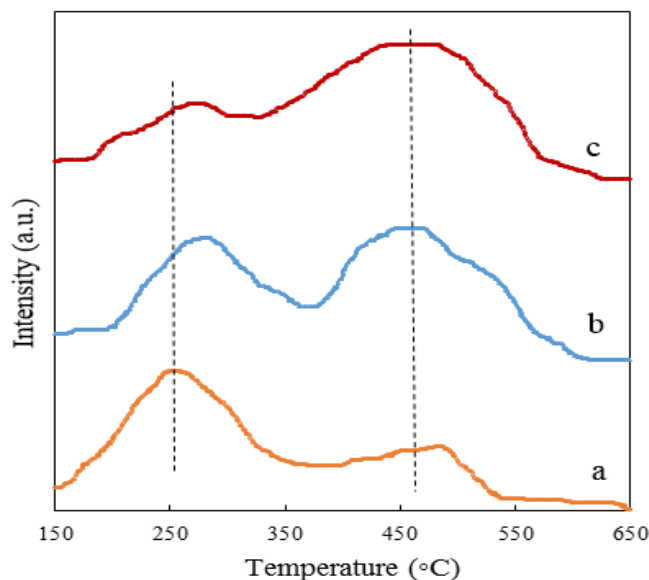

Figure 3

H_2-TPR of 14 wt.% CuOx/OMWNT's calcined at a) 300 °C, b) 500 °C, and c) 700 °C.

The SEM-EDS analysis of the CuOx /OMWNT's (14 wt.%) calcined at 300 °C for 3 hrs is illustrated in Figure 4. The SEM image shows that the impregnation method has provided a good dispersion of nanoparticles over the surface of the OMWNT's. From EDS spectrum, it was observed that the atomic ratio of Cu to O is (2.22/1.82) 1.22>1, indicating the presence of CuO as a dominant phase and Cu_2O as a trace phase (Wang et al., 2009); thus, the XRD analysis of the 14 wt.% catalyst calcined at 300 °C for 3 hrs (Figure 2b) could not detect the Cu_2O nanocrystallines.
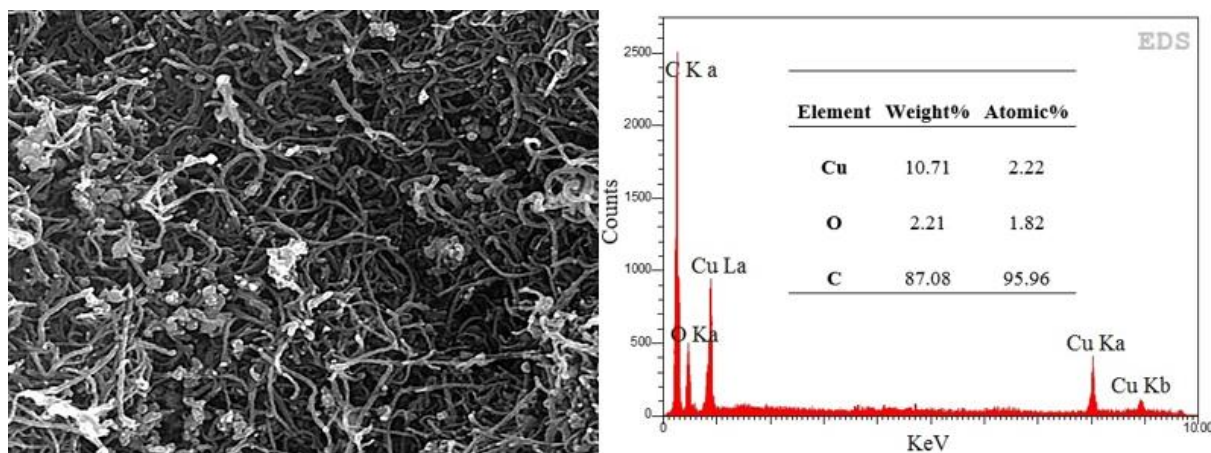

Figure 4

SEM /EDS image of the 14 wt.% CuOx/OMWNT's calcined at 300 °C for 3 hrs.

3.2. Response surface modeling using central composite design

Based on the experimental results presented in Table 2, the second-order polynomial equation in terms of actual factors (Equation 3) was derived to demonstrate the relationship between the independent variables and the response function.

$$Y = -22.63011 + (0.10024)A + (3.12983)B + (10.35364)C + (-7.8125E - 004)AB \\ + (-9.37500E - 004)AC + (-0.096875)BC + (-1.61932E - 004)A^2 \\ + (-0.18608)B^2 + (-0.027477)C^2 \quad (3)$$

In order to assess the accuracy of the model, the analysis of variance (ANOVA) was applied (Amin and Solaimany Nazar, 2016), and the empirical second-order polynomial parameters are presented in Table 3. The F-value of 120.29 implies that the model is highly significant. The model p value is smaller than 0.0001, which also indicates that the model is significant. The "lack of fit F-value" of 4.95 implies that the lack of fit is not significant relative to the pure error. The non-significant lack-of-fit confirms the good predictability of the model. The "Predicted R-squared" of 0.9317 is in reasonable agreement with the "Adjusted R-squared" of 0.9826, which supports an excellent predictability of the model. "Adequate Precision" measures the signal to noise ratio, and a ratio greater than 4 is desirable. In this model, the ratio is 33.858, which indicates an adequate signal.

Table 3

ANOVA results for NOx removal process.

Sources	SS	DF	MS	F-value	p-value-probability > F	Remarks
Model	11090.69	9	1232.30	120.29	<0.0001	Significant
A: Temperature	2528.10	1	2528.10	246.78	<0.0001	
B: Time	115.60	1	115.60	11.28	0.0073	
C: Loading	2592.10	1	2592.10	253.02	<0.0001	
AB	3.13	1	3.13	0.31	0.5929	
AC	28.13	1	28.13	2.75	0.1285	
BC	120.13	1	120.13	11.73	0.0065	
A²	115.38	1	115.38	11.26	0.0073	
B²	24.38	1	24.38	2.38	0.1540	
C²	2076.25	1	2076.25	202.67	<0.0001	
Residual	102.45	10	10.24			
Lack of fit	85.24	5	17.05	4.95	0.0519	Not significant
Pure error	17.21	5	3.44			
Total	11193.14	19				
R^2=0.9908	Adjusted-R^2=0.9826		Predicted-R^2=0.9317		Adequate Precision=33.858	

Furthermore, Figure 5 shows the predicted values of the model response against the experimental values, where the points have been distributed near the straight line confirming that the actual values well match the predicted values (Kumar and Singh, 2014).
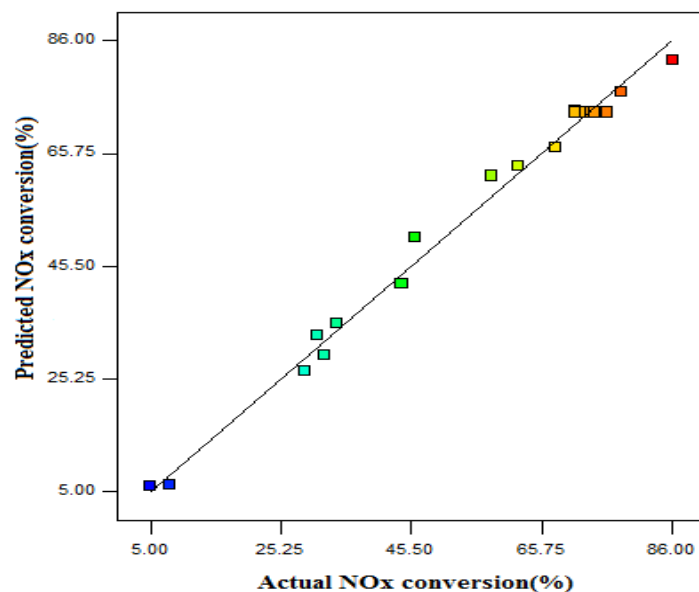
Figure 5

Plot of the actual versus the predicted values of response function.

In the present study, the independent variables, including calcination temperature value (A), CuOx loading (C), and the second order effect of CuOx loading (C^2) are highly significant parameters because of $p < 0.001$. Furthermore, calcination time (B), the second order effect of calcination temperature (A^2), and the interaction of calcination time and CuOx loading (BC) are significant with $p < 0.05$. Moreover, the value of $p > 0.05$ means that the model parameters are insignificant, so Table 3 confirms that AB, AC, and B^2 parameters are insignificant. In order to make an empirical study about the effect of each independent variable, the three dimensional (3D) surfaces were designed representing the conversion of NOx as a function of two variables, while the other variables are kept constant at the central level (Figure 6).
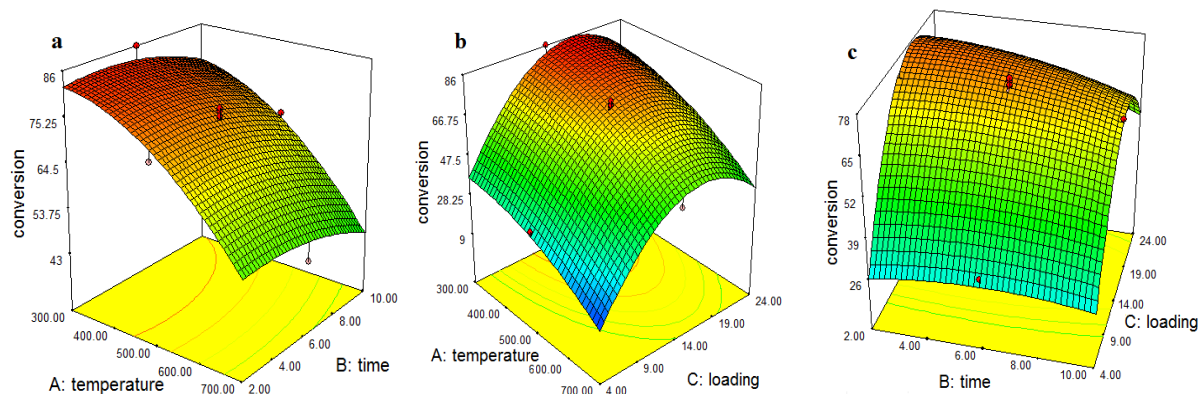

Figure 6

Response surface and contour plots for NOx conversion: a) effects of calcination temperature and calcination time; b) effects of calcination temperature and CuOx loading; and c) effects of calcination time and CuOx loading.

Figure 6a illustrates the effect of calcination temperature (A) and calcination time (B) on NOx conversion. It is observed that NOx conversion is enhanced by lowering calcination temperature from 700 to 300 °C and calcination time from 10 to 2 hrs. It is also obvious that both of these two independent variables are important in conversion response; however, the effect of calcination temperature is far more than calcination time as stated by their p-values. The maximum NOx conversion at a low calcination temperature and time could be attributed to the formation of Cu^{+2} instead of Cu^{+1} and Cu^0 as confirmed by the XRD and H_2-TPR results (Figures 2 and 3).

Figure 6b shows the effects of calcination temperature (*A*) and CuOx loading (*C*). As it can be seen, changing the CuOx loading from 4 to 14 wt.% results in improved conversion due to an increased number of active sites over the surface of the support, whereas further loading to 24 wt.% reduced the conversion. This may be ascribed to the agglomeration of CuOx nanoparticles on the OMWNT's (Pourkhalil et al., 2013). From Figure 6c showing the effects of calcination time and CuOx loading, it is observed that the effect of time at higher at high loadings, so increasing the calcination time and metal loading to respectively more than 2 hrs and 14 wt.% can create greater agglomeration of CuOx active phase.

3.3. Optimization of process conditions using desirability function

The optimization process using Design Expert 7.0.0 was performed on the basis of desirability function to determine the optimum conditions of the independent factors for maximum NOx conversion. The software program has five options, namely none, maximum, minimum, target, and within range, for variables and response factor to obtain the value of 1.00 for desirability function. The conditions for the optimization of all the variables correlated to the NOx conversion are listed in Table 4. The weight or importance factor emphasizes the lower or upper bounds of the variables as well as the target value. Since regarding the maximum conversion is the main goal, the maximum importance of the program, 5, was used (Sakkas et al., 2010) in this study.

Table 4

Optimization of the individual responses (*Y*) in order to find the overall desirability response (*D*).

Name	Goal	Lower limit	Upper limit	Lower weight	Upper weight	Importance
A: Calcination temperature (°C)	In the range	300	700	1	1	3
B: Calcination time (hr.)	In the range	2	10	1	1	3
C: CuOx loading (wt.%)	In the range	4	24	1	1	3
Y: NOx conversion (%)	Maximize	5	86	1	1	5

Based on the above described settings and boundaries, the optimum values of the independent variables for the maximum NOx conversion (86.3%) were 318.4 °C, 3.40 hrs, and 16.73 wt.% for the calcination temperature, calcination time, and copper oxide loading respectively (see Figure 7).
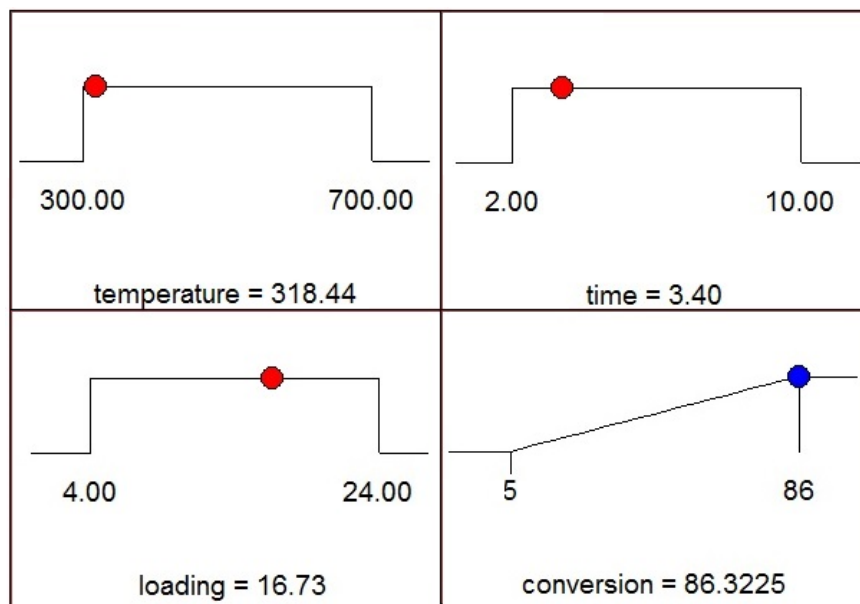

Figure 7

Desirability ramp for the numerical optimization.

4. Conclusions

In the present work, a series of CuOx catalysts supported by OMWNT's were synthesized via a facile method and optimized for the NH$_3$-SCR of nitrogen oxides emitted from low temperature stationary sources (T≈ 200 °C) such as incinerators, shaft furnaces, and electric power plants. The experimental design methodology based on central composite design was utilized to model and optimize the factors influencing the preparation conditions of CuOx/OMWNT's catalysts. A quadratic polynomial model was used to express the functional relationship between NOx conversion as a response factor and three independent variables, including calcination temperature, calcination time, and copper oxide loading. Under the optimized conditions of a calcination temperature of 318.4 °C, a calcination time of 3.40 hrs, and CuOx loading of 16.73 wt.%, an NOx conversion of 86.32% was obtained. The regression analysis with an R^2 value of 0.9908 revealed good agreement between the experimental results and the predicted values. The resistance of NOx catalysts to sulfur dioxide, water vapor, and carbon monoxide poisoning is a serious challenge in different industrial applications. Therefore, future research will be required to investigate and improve the catalyst performance and stability in the presence of H$_2$O, SO$_2$, and CO at low reaction temperatures (T< 250 °C) and at different concentrations of these pollutants.

Acknowledgement

Nomenclature

Adeq. *R*-squared	Adequate R^2
Adj. *R*-squared	Adjust R^2
ANOVA	Analysis of variance
CCD	Central composite design
CuOx	Copper oxide
CVD	Chemical vapor deposition
EDS	Energy dispersive X-ray spectroscopy
FCCCD	Face-centered central composite design
FTIR	Fourier-transform infrared spectroscopy
GHSV	Gas hourly space velocity
H$_2$-TPR	H$_2$-temperature-programmed reduction
JCPDS	Joint Committee on Powder Diffraction Standards
NOx	Nitrogen oxide
OMWNT's	Oxidized multi-walled carbon nanotubes
Pred. *R*-squared	Predicted R^2
RSM	Response surface methodology
SCR	Selective catalytic reduction
SEM	Scanning electron microscopy
XRD	X-ray powder diffraction

References

Amin, F. and Solaimany Nazar A. R., Assessing the Asphaltene Adsorption on Metal Oxide Nanoparticles, Iranian Journal of Oil & Gas Science and Technology, Vol. 5, p. 62-72, 2016.

Badday, A. S., Abdullah A. Z., and Lee K. T., Optimization of Biodiesel Production Process from Jatropha Oil Using Supported Heteropolyacid Catalyst and Assisted by Ultrasonic Energy, Renewable Energy, Vol. 50, p. 427-432, 2013.

Barreau, M., Tarot, M. L., Duprez, D., Courtois, X., and Can, F., Remarkable Enhancement of the Selective Catalytic Reduction of NO at Low Temperature by Collaborative Effect of Ethanol and NH_3 Over Silver Supported Catalyst, Applied Catalysis B: Environmental, Vol. 220, p. 19-30, 2018.

Bazarganipour, M. and Salavati-Niasari, M., Synthesis, Characterization and Chemical Binding of a Ni(II) Schiff Base Complex on Functionalized MWNT's; Catalytic Oxidation of Cyclohexene with Molecular Oxygen, Chemical Engineering Journal, Vol. 286, p. 259-265, 2016.

Belin, T. and Epron, F., Characterization Methods of Carbon Nanotubes: a Review, Materials Science and Engineering: B, Vol. 119, p. 105-118, 2005.

Chuang, K.H., Lu, C.Y., Wey M.Y., and Huang, Y.N., NO Removal by Activated Carbon-supported Copper Catalysts Prepared by Impregnation, Polyol, and Microwave Heated Polyol Processes, Applied Catalysis A: General, Vol. 397, p. 234-240, 2011.

Danmaliki, G. I., Saleh T. A., and Shamsuddeen, A. A., Response Surface Methodology Optimization of Adsorptive Desulfurization on Nickel/Activated Carbon, Chemical Engineering Journal, Vol. 313, p. 993-1003, 2017.

Fang, D., He, F., Liu, X., Qi, K., Xie, J., Li F., and Yu, C., Low Temperature NH_3-SCR of NO over an Unexpected Mn-based Catalyst: Promotional Effect of Mg Doping, Applied Surface Science, Vol. 427, p. 45-55, 2018.

Gangupomu, R. H., Sattler M. L., and Ramirez, D., Comparative Study of Carbon Nanotubes and Granular Activated Carbon: Physicochemical Properties and Adsorption Capacities, Journal of Hazardous Materials, Vol. 302, p. 362-374, 2016.

Hosseini, S. A., Nouri, S. Hashemi S., and Akbari, M., Investigation of Performance of Ni/Clinoptilolite Nanoadsorbents in Desulfurization of Gas Oil: Experimental Design and Modeling, Iranian Journal of Oil & Gas Science and Technology, Vol. 6, p. 13-25, 2017.

Jiang, L. and Gao, L., Modified Carbon Nanotubes: An Effective Way to Selective Attachment of Gold Nanoparticles, Carbon, Vol. 41, p. 2923-2929, 2003.

Jung, H., Park, E., Kim M., and Jurng, J., A Pilot-scale Evaluation of a Novel TiO_2-supported V_2O_5 Catalyst for Denox at Low Temperatures at a Waste Incinerator, Waste Management, Vol. 61, p. 283-287, 2017.

Jung, Y., Shin, Y. J., Pyo, Y. D., Cho, C. P., Jang J., and Kim, G., NOx and N_2O Emissions over a Urea-SCR System Containing both V_2O_5-WO_3/TiO_2 and Cu-Zeolite Catalysts in a Diesel Engine, Chemical Engineering Journal, Vol. 326, p. 853-862, 2017.

Kibria, A. K. M. F., Shajahan, M., Mo, Y. H., Kim M. J., and Nahm, K. S., Long Activity of Co–Mo/MgO Catalyst for the Synthesis of Carbon Nanotubes in Large-scale and Application Feasibility of the Grown Tubes, Diamond and Related Materials, Vol. 13, p. 1865-1872, 2004.

Kumar, S. and Singh, R. K., Optimization of Process Parameters by Response Surface Methodology (RSM) for Catalytic Pyrolysis of Waste High-density Polyethylene to Liquid Fuel, Journal of Environmental Chemical Engineering, Vol. 2, p. 115-122, 2014.

Li, Q., Yang, H., Ma Z., and Zhang, X., Selective Catalytic Reduction of NO with NH_3 over CuOx-Carbonaceous Materials, Catalysis Communications, Vol. 17, p. 8-12, 2012.

Liu, M., Yang, Y., Zhu T., and Liu, Z., Chemical Modification of Single-walled Carbon Nanotubes with Peroxytrifluoroacetic Acid, Carbon, Vol. 43, p. 1470-1478, 2005.

Liu, X., Wu, X., Weng D., and Shi, L., Modification of Cu/ZSM-5 Catalyst with CeO_2 for Selective Catalytic Reduction of NOx with Ammonia, Journal of Rare Earths, Vol. 34, p. 1004-1009, 2016.

Luo, J., Gao, F., Kamasamudram, K., Currier, N., Peden C. H. F., and Yezerets, A., New Insights into Cu/SSZ-13 SCR Catalyst Acidity, Part I: Nature of Acidic Sites Probed by NH_3 Titration, Journal of Catalysis, Vol. 348, p. 291-299, 2017.

Lv, J., Li, D., Dai, Liang, C., Jiang, D., Lu L., and Zhu, G., Multi-walled Carbon Nanotube Supported Cd's-DETA Nanocomposite for Efficient Visible Light Photocatalysis, Materials Chemistry and Physics, Vol. 186, p. 372-381, 2017.

Pourkhalil, M., Izadi, N., Rashidi, A., and Mohammad-Taheri, M., Synthesis of $CeOx/\Gamma-Al_2O_3$ Catalyst for the NH_3-SCR of NOx, Materials Research Bulletin, Vol. 97, p. 1-5, 2018

Pourkhalil, M., Moghaddam, A. Z., Rashidi, A., Towfighi, J., and Mortazavi, Y., Preparation of Highly Active Manganese Oxides Supported on Functionalized MWNT's for Low Temperature NOx Reduction with NH_3, Applied Surface Science, Vol. 279, p. 250-259, 2013.

Roe, D. P., Xu R., and Roberts, C. B., Influence of a Carbon Nanotube Support and Supercritical Fluid Reaction Medium on Fe-catalyzed Fischer-Tropsch Synthesis, Applied Catalysis A: General, Vol. 543, p. 141-149, 2017.

Sakkas, V. A., Islam, M. A., Stalikas C., and Albanis, T. A., Photocatalytic Degradation Using Design of Experiments: A Review and Example of The Congo Red Degradation, Journal of Hazardous Materials, Vol. 175, p. 33-44, 2010.

Samojeden, B., Motak, M., and Grzybek, T., The Influence of the Modification of Carbonaceous Materials on their Catalytic Properties in SCR-NH_3: A Short Review, Comptes Rendus Chimie, Vol. 18, p. 1049-1073, 2015.

Sedaghatzadeh, M., Khodadadi, A., and Tahmasebi Birgani, M. R., An Improvement in Thermal and Rheological Properties of Water-based Drilling Fluids Using Multiwall Carbon Nanotube (MWCNT), Iranian Journal of Oil & Gas Science and Technology, Vol. 1, p. 55-65, 2012.

Shan, Y., Shi, X., Yan, Z., Liu, J., Yu, Y., and He, H., Deactivation of Cu-SSZ-13 in the Presence of SO_2 During Hydrothermal Aging, Catalysis Today, in Press, Corrected Proof, 2017.

Sun, P., Guo, R.T., Liu, S.M., Wang, S.X., Pan, W.G., Li, M.Y., Liu, S.W., Liu, J., and Sun, X., Enhancement of the Low-temperature Activity of Ce/TiO_2 Catalyst by Modification for Selective Catalytic Reduction of NOx with NH_3, Molecular Catalysis, Vol. 433, p. 224-234, 2017.

Vermisoglou, E. C., Romanos, G. E., Karanikolos, G. N., and Kanellopoulos, N. K., Catalytic NOx Removal by Single-wall Carbon Nanotube-supported Rh Nanoparticles, Journal of Hazardous Materials, Vol. 194, p. 144-155, 2011.

Wan, Y., Ma, J., Wang, Z., Zhou, W., and Kaliaguine, S., Selective Catalytic Reduction of NO over Cu-Al-MCM-41, Journal of Catalysis, Vol. 227, p. 242-252, 2004.

Wang, J., Zhao, H., Haller, G., and Li, Y., Recent Advances in the Selective Catalytic Reduction of NOx With NH$_3$ on Cu-Chabazite Catalysts, Applied Catalysis B: Environmental, Vol. 202, p. 346-354, 2017.

Wang, X., Zheng, Y., and Lin J., Highly Dispersed Mn–Ce Mixed Oxides Supported on Carbon Nanotubes for Low-temperature NO Reduction with NH$_3$, Catalysis Communications, Vol. 37, p. 96-99, 2013.

Wu, G., Feng, X., Zhang, H., Zhang, Y., Wang, J., Chen, Y., and Dan, Y., The Promotional Role of Ni in FevO$_4$/TiO$_2$ Monolith Catalyst for Selective Catalytic Reduction of NOx with NH$_3$, Applied Surface Science, Vol. 427, p. 24-36, 2018.

Xing, Y., Li, L., Chusuei, C. C., and Hull, R. V., Sonochemical Oxidation of Multiwalled Carbon Nanotubes, Langmuir, Vol. 21, p. 4185-90, 2005.

Zhang, Y.C., Pan, L., Lu, J., Song, J., Li, Z., Zhang, X., Wang L., and Zou, J.J., Unraveling the Facet-dependent and Oxygen Vacancy Role for Ethylene Hydrogenation on Co$_3$O$_4$ (110) Surface: A DFT+U Study, Applied Surface Science, Vol. 401, p. 241-247, 2017

Zhu, Z., Liu, Z., Liu, S., Niu, H., Hu, T., Liu, T., and Xie, Y., NO Reduction with NH$_3$ over an Activated Carbon-supported Copper Oxide Catalysts at Low Temperatures, Applied Catalysis B: Environmental, Vol. 26, p. 25-35, 2000.